Oscillatory magnetoresistance in the charge-transfer salt β''-(BEDT-TTF)$_2$AuBr$_2$ in magnetic fields up to 60 T: Evidence for field-induced Fermi-surface reconstruction

A. A. House
Department of Physics, University of Oxford, Clarendon Laboratory, Parks Road, Oxford OX1 3PU, United Kingdom

N. Harrison
Laboratorium voor Vaste-Stoffysica en Magnetisme, Katholieke Universiteit Leuven, Celestijnenlaan 200D, B-3001 Heverlee, Belgium

S. J. Blundell
Department of Physics, University of Oxford, Clarendon Laboratory, Parks Road, Oxford OX1 3PU, United Kingdom

I. Deckers
Laboratorium voor Vaste-Stoffysica en Magnetisme, Katholieke Universiteit Leuven, Celestijnenlaan 200D, B-3001 Heverlee, Belgium

J. Singleton
Department of Physics, University of Oxford, Clarendon Laboratory, Parks Road, Oxford OX1 3PU, United Kingdom

F. Herlach
Laboratorium voor Vaste-Stoffysica en Magnetisme, Katholieke Universiteit Leuven, Celestijnenlaan 200D, B-3001 Heverlee, Belgium

W. Hayes
Department of Physics, University of Oxford, Clarendon Laboratory, Parks Road, Oxford OX1 3PU, United Kingdom

J. A. A. J. Perenboom
Laboratorium voor Hoge Magneetvelden, Katholieke Universiteit Nijmegen, Toernooiveld 1, NL 6525 ED Nijmegen, The Netherlands

M. Kurmoo
Department of Physics, University of Oxford, Clarendon Laboratory, Parks Road, Oxford OX1 3PU, United Kingdom and The Royal Institution, 21 Albemarle Street, London W1X 4BS, United Kingdom

P. Day
The Royal Institution, 21 Albemarle Street, London W1X 4BS, United Kingdom
(Received 6 October 1995)

Magnetoresistance measurements carried out in pulsed magnetic fields of up to 60 T and at temperatures down to 350 mK and angle-dependent magnetoresistance experiments performed in quasistatic fields have been used to establish that the charge-transfer salt β''-(BEDT-TTF)$_2$AuBr$_2$ undergoes a change in electronic structure at $\sim$10 T. We propose that this arises due to a field-induced transition between two different spin-density-wave states. Furthermore, at the highest magnetic fields, both the background magnetoresistance and effective masses of the quasiparticles were found to increase, possibly as a result of an enhancement of the density of states. It is found that frequency mixing effects at very high magnetic fields, observed in the Fourier spectra of the magnetoresistance, cannot be explained by the Shoenberg magnetic interaction, but are instead probably caused by oscillations in the chemical potential which become important as the extreme quantum limit is approached.

I. INTRODUCTION

Pulsed magnetic fields of $\sim$50 T have recently proved to be a powerful tool for the study of charge-transfer salts of the ion BEDT-TTF.[1–5] Some of these salts are found to undergo transitions at high magnetic fields between spin-density-wave (SDW) and metallic regimes (Refs. 2–7 and references therein); in addition, the amplitudes of quantum oscillatory phenomena such as the Shubnikov–de Haas (SdH) and de Haas–van Alphen (dHvA) effects are found to grow dramatically with increasing magnetic field and appear to deviate significantly from conventional Lifshitz-Kosevich behavior.[2,3,8] In this paper we have used magnetoresistance measurements in pulsed fields of up to 60 T and the observation of angle-dependent magnetoresistance oscillations in static fields to demonstrate that the charge-transfer salt β''-(BEDT-TTF)$_2$AuBr$_2$ undergoes a field-driven transition between two different SDW ground states.

β''-(BEDT-TTF)$_2$AuBr$_2$ is a particularly interesting material, exhibiting a variety of apparent magnetic phase transitions below 30 K.[9–11] Furthermore, the low-temperature magnetoresistance of typical samples possesses a complex dependence on field strength and orientation,[9] plus a rich spectrum of SdH and dHvA oscillations.[9–11] These have

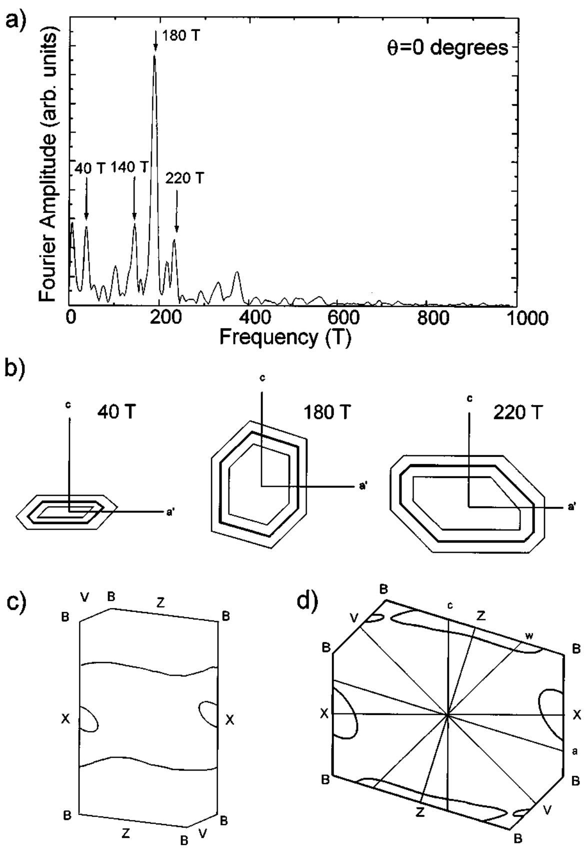

FIG. 1. (a) Fourier spectrum of the SdH oscillations in β''-(BEDT-TTF)$_2$AuBr$_2$ for a field sweep at 490 mK with the magnetic field perpendicular to the ac crystallographic plane [from Doporto *et al.* (Ref. 9)]. Note the peaks occurring at 40, 140, 180, and 220 T. (b) Shapes and orientations of the three Fermi-surface pockets proposed by Doporto *et al.* (Ref. 9) from observation of the angular dependence of the SdH oscillation amplitudes. (c) Section through the first Brillouin zone of β''-(BEDT-TTF)$_2$AuBr$_2$ showing the calculated room-temperature Fermi surface of Mori *et al.* (Ref. 12). (d) Reconstructed Brillouin zone and Fermi surface proposed by Doporto *et al.* (Ref. 9).

proved difficult to reconcile with the various predicted Fermi surfaces, which either consist of quasi-one-dimensional (Q1D) sheets or a single closed Q2D pocket plus a Q1D section [see Fig. 1(c) for one example;[12] for a summary of other calculations, see Fig. 1 of Ref. 9]. Nevertheless, only a very limited number of studies of this material have been carried out (see Refs. 9–11 and references therein), chiefly because of the low yield of crystals of the β'' phase.

Perhaps the most complete study has been that of Doporto *et al.*,[9] which concentrated on the field region below 30 T; the results of that work are summarized in Fig. 1. An examination of the field orientation dependence of the amplitude of the SdH oscillations was used to derive a Fermi surface consisting of three small anisotropic Q2D pockets with area corresponding to SdH frequencies 40, 180, and 220 T [Figs. 1(a) and 1(b)]. One of these pockets was identified with the small Q2D section predicted in the band-structure calculations of Mori *et al.*[12] [Fig. 1(c)], while the others were attributed to an imperfectly nested SDW associated with the Q1D section of the Fermi surface [Fig. 1(d)]. Other SdH frequencies, in particular a strong set of oscillations with frequency 140 T [Fig. 1(a)], were thought to be due to frequency mixing[9] caused by the Shoenberg magnetic interaction.[13]

In this paper angle-dependent magnetoresistance oscillations measured in static fields between 1 and 17 T and magnetotransport carried out in pulsed fields of up to 60 T have been used to demonstrate that, while the Fermi surface proposed by Doporto *et al.*[9] contains some of the elements necessary to account for the behavior of β''-(BEDT-TTF)$_2$AuBr$_2$, the Shoenberg magnetic interaction is insufficiently strong to produce the effects suggested in Ref. 9 and that some of the extra observed SdH frequencies arise from a field-induced phase transition occurring at around 10 T.

II. EXPERIMENTAL DETAILS

The β''-(BEDT-TTF)$_2$AuBr$_2$ samples used in these experiments were distorted hexagonal black platelets with dimensions of approximately $0.5\times0.5\times0.1$ mm^3; the sample growth and preparation details are identical to those described in Ref. 9.

Pulsed field magnetoresistance measurements were performed on two separate samples (A and B) at the Leuven high field facility.[14] The samples were orientated with their conducting (2D) ac planes perpendicular to the magnetic field. Four-wire contacts were made to the samples using platinum paint and 25-μm gold wire, giving typical two-terminal contact resistances of $\sim$50 Ω. All experiments were performed with an alternating current of 10 μA at 250 kHz applied perpendicular to the conducting ac planes (see Ref. 9 for a discussion concerning the choice of this current direction). The voltage signal was preamplified and subsequently detected using a fast lock-in amplifier. The integration time on the lock-in amplifier was set to 10 μs so that real-time frequencies in the magnetoresistance of up to 20 kHz could be detected without any noticeable attenuation. This enabled magnetoresistance oscillations to be measured on the falling (i.e., lower dB/dt) side of the field pulse[14] down to the lowest magnetic fields. Fields of up to 60 T were applied to the sample, while temperatures down to 350 mK were provided by means of a plastic ^{3}He insert. Owing to the relatively large resistivity of this material and small sample size, eddy current heating[2] was not significant; this fact was established by comparing magnetoresistance data recorded with different field pulse heights.[2] The cryostat was mechanically decoupled from the pulsed magnet to minimize the effects of vibrational noise.

The angle-dependent magnetoresistance oscillations were measured for a third sample (C) in static fields of up to 17 T provided by a Bitter magnet at Nijmegen. The sample was placed in a cryostat, which allowed it to be rotated about two perpendicular axes *in situ* with a precision of $\pm1°$. Cooling was provided by ^{4}He exchange gas, allowing the temperature range between 4.2 and 1.5 K to be studied. The crystal was aligned by measuring the polarized infrared reflectivity at room temperature. Contacts were made in the same manner as for the pulsed field experiments and the measurement was performed using standard four-wire ac techniques (20–130 Hz), with the current directed perpendicular to the ac planes. The magnitude of the current was 20 μA throughout the experiment.

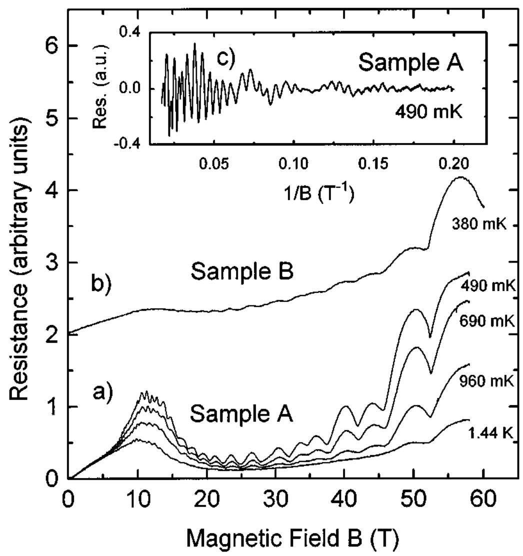

FIG. 2. (a) Magnetoresistance of sample A of β''-(BEDT-TTF)$_2$AuBr$_2$ for temperatures in the range 490 mK to 1.44 K. (b) Magnetoresistance of sample B of β''-(BEDT-TTF)$_2$AuBr$_2$ at 380 mK. (c) Oscillatory component of the 490 mK trace of (a) derived using division by an exponential polynomial approximation to the classical background magnetoresistance.

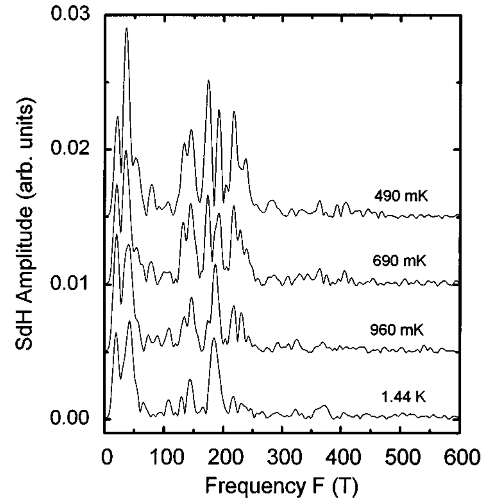

FIG. 3. Fourier spectra of the data presented in Fig. 2(a), after the appropriate removal of the background magnetoresistance [as demonstrated in Fig. 2(c)].

III. MAGNETORESISTANCE

A. General features and Shubnikov–de Haas oscillations

Figures 2(a) and 2(b) show measured magnetoresistance traces for the samples A and B on the falling side of the field pulse. The magnetoresistance oscillations measured in sample A were larger than in sample B, perhaps because of better sample quality. The analysis of the quantum oscillations in this paper therefore concentrates on sample A, although sample B was found in all other respects to behave in a similar manner.

We first turn to the classical background magnetoresistance (as opposed to the oscillatory SdH component) of β''-(BEDT-TTF)$_2$AuBr$_2$; experimental traces at several different temperatures are shown for sample A in Fig. 2(a). The behavior of the low-field magnetoresistance is in good agreement with previous measurements on these and other samples in static magnetic fields of up to 20 T;[9] it exhibits a relatively temperature-independent, almost linear, rise to ~6 T followed by a steeper rise to about 10 T. Above this field the magnetoresistance undergoes a drastic change in gradient, falling to a minimum at about 25 T, before increasing steeply again. At all fields above 6 T, the magnetoresistance depends strongly on temperature.

The supposed presence of a SDW in β''-(BEDT-TTF)$_2$AuBr$_2$ (see Ref. 9 and references therein for a discussion of the experimental evidence for a SDW ground state) and the observation of drastic changes in magnetoresistance gradient invite immediate comparisons with α-(BEDT-TTF)$_2M$Hg(SCN)$_4$ (M=K, Tl, Rb). The latter materials are also thought to exhibit SDW ground states and show strong "kinks" in the magnetoresistance,[1–4,7,15,16] commonly associated with the destruction of the SDW due to the applied field. Part of the evidence for this is drawn from the fact that below ~5 K the classical background magnetoresistances of the α-(BEDT-TTF)$_2M$Hg(SCN)$_4$ (M=K, Tl, Rb) salts are strongly temperature dependent at fields below the "kink" (i.e., in the SDW state), but virtually temperature independent at fields above it (i.e., in the metallic state) (see Refs. 1–4, 7, 15, and 16 and references therein). The fact that the low-temperature magnetoresistance of β''-(BEDT-TTF)$_2$AuBr$_2$ is strongly temperature dependent up to the highest available field [Fig. 2(a)] therefore suggests that this material continues to remain in a SDW state up to 60 T for the temperature range examined in this study.

We turn to the oscillatory (SdH) component of the magnetoresistance of β''-(BEDT-TTF)$_2$AuBr$_2$. Previous studies on this material have shown hysteresis in the magnetoresistance at fields below ~20 T.[9] This effect was also observable in the present experiments, but for fields below ~15 T on the rising side of the pulse, the oscillatory component of the magnetoresistance suffered some degree of attenuation as a result of sampling problems of the lock-in amplifier during the region of high dB/dt at the start of each pulse.[2,14] For this reason the analysis of the quantum oscillations is restricted to the falling side of the pulse.

For the purpose of the analysis, $\rho(1/B)$, the oscillatory component of the magnetoresistance, was divided by the classical background magnetoresistance $P(1/B)$ in reciprocal magnetic field space. $P(1/B)$ was approximated to an exponential polynomial of the form $P=\exp\{a_0+a_1/B+a_2/B^2+\cdots\}$. Figure 2(c) shows the resulting oscillatory component of the magnetoresistance; the Shubnikov–de Haas oscillations can be clearly observed down to magnetic fields of around 5 T. Spectral analyses of the data in Figs. 2(c) and other experimental traces at different temperatures are shown in Fig. 3; Hanning windows[13] were applied to all data sets prior to Fourier transformation. As the measurements were performed over an extensive range in $1/B$ space (from 0.017 to ~0.2 T^{-1}), SdH frequencies can be distinguished with an absolute resolution of ~10 T. The transformed data exhibit rich spectra of SdH frequencies with a much more complex form than earlier published results;[9,10] in previous low-field studies (to ~20 T), where the magnetoresistance or magnetization has been measured using standard techniques, the Fourier spectra have been found to be dominated by four principal frequencies, ~40, ~140, ~180, and ~220 T [see, e.g., Fig. 1(a)]. In Fig. 3 the previously known frequencies of 140 and 180 T appear to be split into separate frequencies of 133 and 145 T, and 175 and ~195 T, respectively. Additional features are also present at ~53 and 240 T, whereas the frequencies at ~77 and 108 T are almost certainly second harmonics. The feature at ~20 T is an artifact of the background polynomial subtraction. At higher temperatures, as is apparent in Fig. 3, the 195 T frequency drops strongly in amplitude to reveal a further frequency at ~185 T. While there appear to be many new features in this data, the frequencies at 38 and 218 T are in accord with values reported in previous studies.[9,10]

The presence of apparent additive relationships between the components of the Fourier spectra has previously been interpreted as originating from the Shoenberg magnetic interaction.[9,11] It has been speculated that this effect might also account for some of the SdH frequencies observed in α-(BEDT-TTF)$_2$KHg(SCN)$_4$.[15] However, recent absolute amplitude measurements of the dHvA effect in α-(BEDT-TTF)$_2$KHg(SCN)$_4$ at high magnetic fields[2] have shown that the internal fields are too small by at least four orders of magnitude. As the SdH frequencies in β''- (BEDT-TTF)$_2$AuBr$_2$ are even lower than those of α-(BEDT-TTF)$_2$KHg(SCN)$_4$ (cf. Ref. 2 and this work), the internal fields generated by the oscillatory magnetization will be much smaller in β''-(BEDT-TTF)$_2$AuBr$_2$.[2,13] Considered in the framework of the Lifshitz-Kosevich model for the amplitude of dHvA oscillations in a metal,[13] it is now clear that the magnetic interaction is not a significant effect in β''-(BEDT-TTF)$_2$AuBr$_2$.

Since magnetic interaction is ruled out as an explanation of the multiple frequencies in β''-(BEDT-TTF)$_2$AuBr$_2$, another explanation must be sought. Figure 4(a) shows the first differential of the magnetoresistance with respect to the magnetic field, obtained by numerical differentiation of raw data such as those in Fig. 2(a). In Fig. 4(b) this procedure has also been applied to magnetoresistance data recorded using a Bitter magnet and taken from Ref. 9, with a higher signal-to-noise ratio at the lowest magnetic fields. The dominant SdH frequencies over various field ranges are shown in Fig. 4(c), which displays the index of each oscillation minimum versus the reciprocal magnetic field.

From Fig. 4(c) it is clear that in the region 0.017–0.1 T^{-1} (~10–60 T), a SdH frequency $F_{\gamma'}\approx 222$ T dominates the oscillatory component of the magnetoresistance, interfering with weaker SdH oscillations of other frequencies. In the region 0.1–0.16 T^{-1} (6.3–10 T), a frequency $F_\gamma \approx 191$ T is strongest, until finally in the field region 0.16–0.25 T^{-1} (~4–6.3 T) the magnetoresistance minima correspond to a frequency $F_\beta \approx 143$ T. A detailed Fourier analysis of the quantum oscillations over different field ranges reveals that the $F_{\gamma'}\approx 222$ T frequency appears only above 10 T, while the $F_\gamma \approx 191$ T frequency (which dominates the magnetoresistance between 6 and 10 T) vanished above ~14 T.

The Fourier transforms in Figs. 5(a) (above 14 T) and 5(b) (below 10 T) also show very clearly that different sets of SdH frequencies are present at high and low magnetic fields. At fields below 10 T three frequencies $F_\alpha \approx 38$ T, $F_\beta \approx 143$ T,

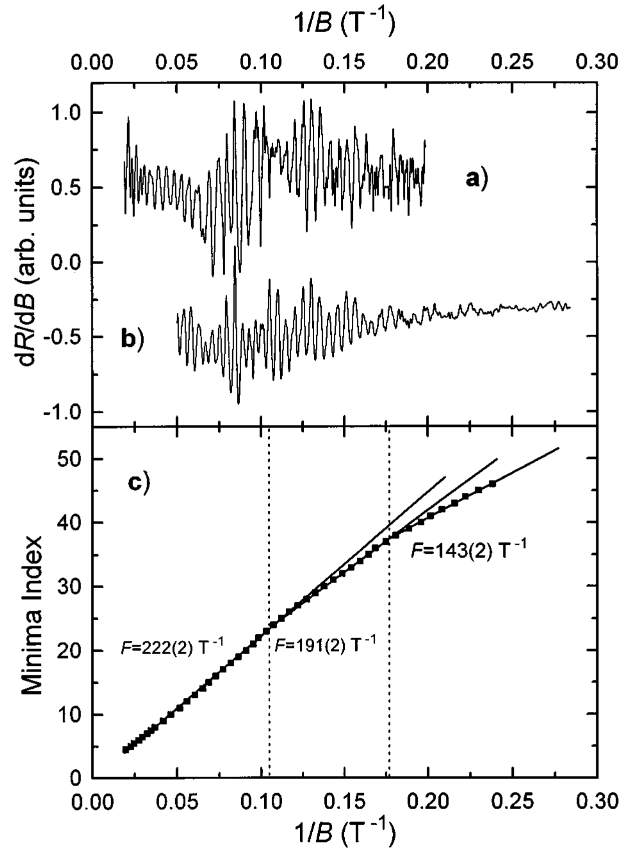

FIG. 4. (a) First differential of the magnetoresistance with respect to magnetic field for raw pulsed field data, such as that of Fig. 2(a). (b) First differential of the magnetoresistance with respect to magnetic field for raw data obtained using a Bitter magnet by Doporto *et al.* (Ref. 9). (c) Landau level index of the SdH oscillation minima plotted against reciprocal magnetic field. This figure shows the reciprocal field regions over which different SdH frequencies dominate the Fourier spectrum.

and $F_\gamma \approx 191$ T are prominent [cf. Figs. 5(b) and 4(c)], whereas above 14 T, $F_\alpha \approx 38$ T, $F_{\beta'} \approx 175$ T, and $F_{\gamma'} \approx 222$ T dominate [cf. Figs. 5(a) and 4(c)]. In the intermediate region between 10 and 14 T, a poorly resolved mixture of frequencies is observed [Fig. 5(a), inset].

When performing Fourier transforms it was found that the modulation of the data by the Hanning window led to the introduction of an extra low-frequency component to the resulting Fourier spectra. For transforms taken across the entire field range, this effect was negligible, but for analysis over smaller regions of reciprocal space, this artificial peak became more significant and led to distortion of the low-frequency $F_\alpha \approx 38$ T SdH peak, thus shifting it to a lower frequency value. It was necessary to retain the use of a window function in order to avoid spurious peaks at higher frequencies on the Fourier transform, but it should be noted that the values that have been derived for the F_α frequency were obtained by performing a Fourier transformation in the absence of any apodization.

It is worth remarking that similar transforms to that in Fig. 5(b) were obtained by Uji *et al.* using a field-modulation method to enhance the oscillatory component of the magnetoresistance.[10,17] The reason for the plethora of fre-

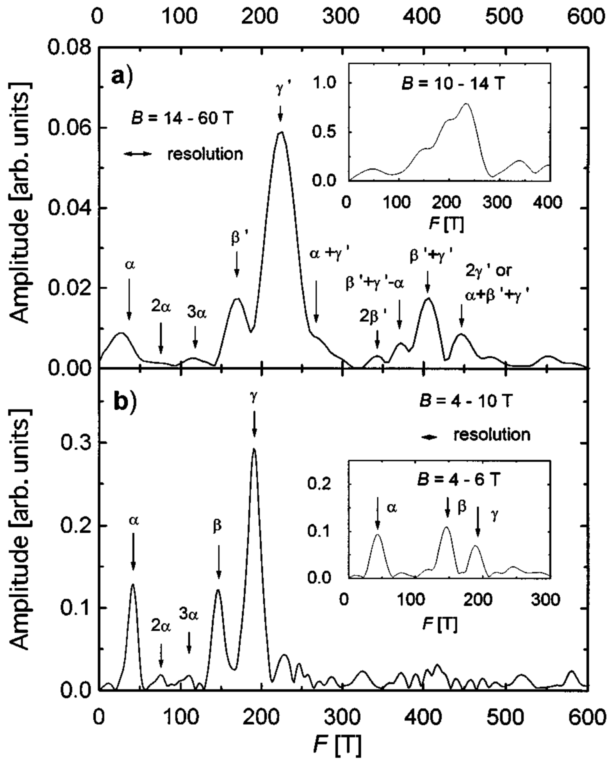

FIG. 5. (a) Fourier spectrum taken over the field region from 14 to 60 T. Note the prominent peaks at $F_{\alpha}\approx 38$ T, $F_{\beta'}\approx 175$ T, and $F_{\gamma'}\approx 222$ T. (b) Fourier spectrum for the field region 4–10 T. In this case the dominant spectral peaks are observed to be $F_{\alpha}\approx 38$ T, $F_{\beta}\approx 143$ T, and $F_{\gamma}\approx 191$ T.

quencies in the Fourier transform of the complete field range (Fig. 3) is now apparent; different SdH frequencies dominate the oscillatory component of the magnetoresistance over different field ranges. In order to clarify the changes in Fermi-surface topology which gives rise to this phenomenon, we turn to the angle-dependent magnetoresistance oscillations of β''-(BEDT-TTF)$_2$AuBr$_2$.

B. Angle-dependent magnetoresistance oscillations

The technique of observing magnetoresistance as a sample is rotated in a constant magnetic field has become a powerful tool for deducing the Fermi-surface (FS) topology of organic metals. Both Q1D and Q2D sections of the FS can cause angle-dependent magnetoresistance oscillations (AMRO's) via two different mechanisms; it is the Q2D mechanism which is thought to be important in β''-(BEDT-TTF)$_2$AuBr$_2$.[9] AMRO peaks due to a warped Q2D Fermi surface have been thoroughly treated in Ref. 18 and are connected with the vanishing of the electronic group velocity perpendicular to the 2D layers. The angles between the normal to the 2D planes and the magnetic field, θ_i, at which the maxima occur are given by

$$b' k_{\parallel}\tan(\theta_i)=\pi(i\pm\tfrac{1}{4})+A(\varphi), \tag{1}$$

where the signs $-$ and $+$ correspond to positive and negative θ_i, respectively, b' is the effective interplane spacing, $k_{\parallel}$ is the maximum Fermi wave-vector projection on the plane of rotation of the field, and $i=\pm 1,\pm 2,\ldots$.[18] Here positive i correspond to $\theta_i>0$ and negative i to $\theta_i<0$. The gradient of a plot of $\tan(\theta_i)$ against i may thus be used to find one of the dimensions of the Fermi surface, and if the process is repeated for several planes of rotation, defined by an azimuthal angle φ, the complete Fermi surface can be mapped.[15,18] (φ is defined to be zero in the direction perpendicular to the crystallographic c axis in the ac plane). $A(\varphi)$ is a function of the plane of rotation of the field, determined by the inclination of the plane of warping; hence, this may also be found.[18]

Figure 6(a) shows the magnetoresistance plotted as a function of tilt angle θ. Note that most of the features in the magnetoresistance do not shift as B is increased, but merely grow in amplitude; this is characteristic of AMRO's, which depend on the classical trajectories of the electrons across the Fermi surface.[15,18,19] However, for $B>\sim 10$ T a new series of strong oscillations grows, indicating that the Fermi surface has changed in form. Note that one set of AMRO's is observed close to 90° at all magnetic fields and has a period $\Delta(\tan(\theta))$ of between 2 and 4, depending on the azimuthal angle φ [Fig. 6(b)]; such a large value indicates a small Fermi-surface pocket, which we shall label the α pocket. On the other hand, the AMRO's which appear for fields above 10 T [Fig. 6(a)] have a smaller period in $\tan\theta$, indicating that they are associated with a larger area Q2D pocket. Their appearance at the same field as the $F_{\gamma'}\approx 222$ T frequency SdH oscillations [see Figs. 4(a) and 5(a)] strongly suggests that the two phenomena are associated with the same Fermi-surface pocket. We shall refer to this section of Fermi surface as the γ' pocket.

Assuming for simplicity that the Fermi-surface pockets involved possess elliptical cross sections, the projection vector $k_{\parallel}$ (normal to the tangent) is related to the radii of the major semi axis k_x and minor semiaxis k_y of a particular ellipse by

$$k_{\parallel}=[k_x^2\cos^2(\varphi-\xi)+k_y^2\sin^2(\varphi-\xi)]^{1/2}, \tag{2}$$

where φ is again (see above) the azimuthal angle describing angular position in the plane of the ellipse and ξ is the inclination of the major axis with respect to $\varphi=0$. For an elongated ellipse Eq. (2) describes a locus in the form of a figure 8 in polar $k_{\parallel}\varphi$ space, as shown in Fig. 7(a).

Figure 7(b) shows a polar plot of $k_{\parallel}$ derived from the periodicity of the AMRO's close to $\theta=0$ in Fig. 6(b), to which Eq. (2) has been fitted, plus the shape of the derived elliptical Fermi-surface cross section. The AMRO's which emerge above $\sim$10 T indicate that the γ' pocket ($F_{\gamma'}\approx 222$ T SdH frequency) is very elongated, with its long axis perpendicular to the crystallographic c direction. The limited azimuthal resolution of the AMRO experiments means that the length of the short axis k_y cannot be determined to any reasonable accuracy; furthermore, the width determined for this elongated section of Fermi surface will also be prone to error if the pocket is not perfectly elliptical. For these reasons, the AMRO data were fitted using k_x and ξ as adjustable parameters, but with the ellipse area constrained to correspond to a SdH frequency of 222 T. This fit is presented in Fig. 7(b) and yields values of $k_x\approx(4.32\pm 0.07)\times 10^9$ m^{-1} and $k_y\approx 1.6\times 10^8$ m^{-1}. The total length of the major axis of the ellipse, $2k_x$, exceeds the width (7.28×10^9 m^{-1}) of the room-temperature Brillouin zone [Fig. 1(c)]. Since the major axis of this elliptical pocket is inclined at $(-12\pm 2)°$ to the reciprocal lattice

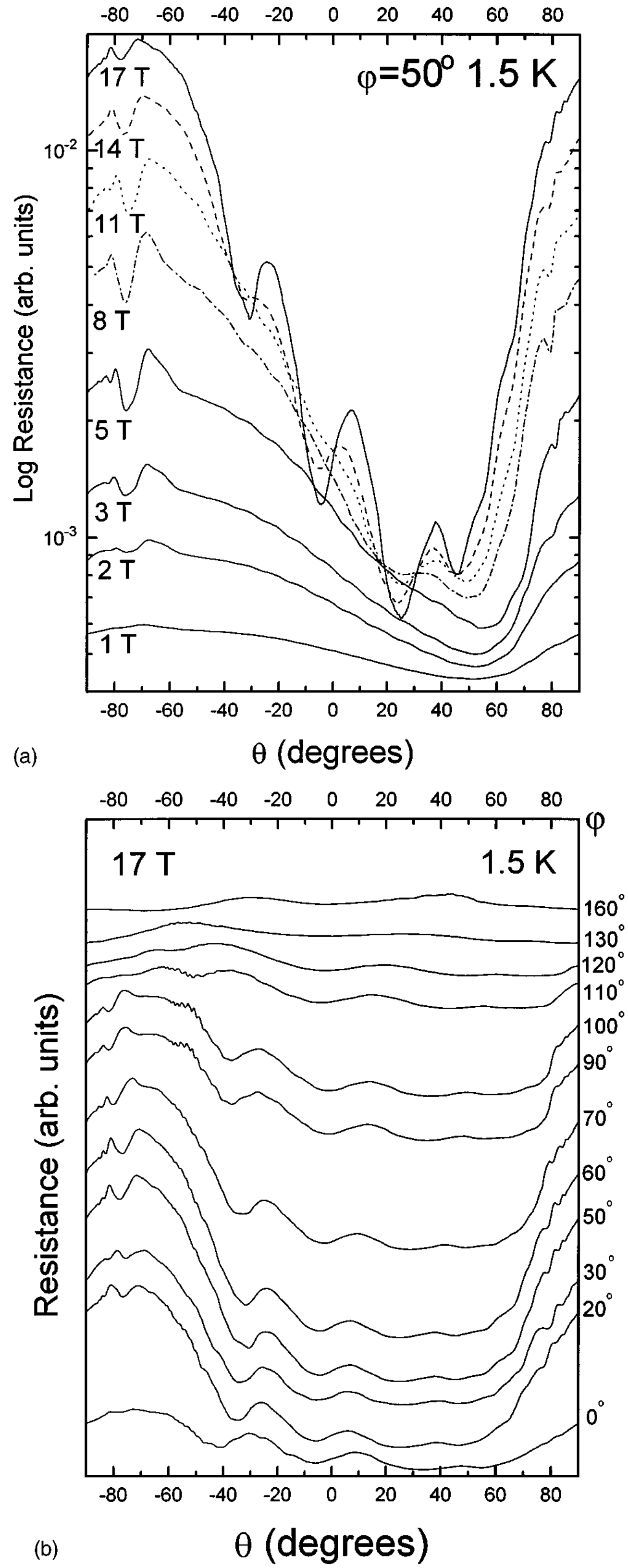

FIG. 6. (a) Field dependence of the AMRO's in β''-(BEDT-TTF)$_2$AuBr$_2$ for φ=50° and 1.5 K. For clarity the 8, 11, and 14 T traces are shown as dot-dashed, dotted, and dashed lines, respectively. (b) Variation of the AMRO's with azimuthal angle φ at 17 T and 1.5 K.

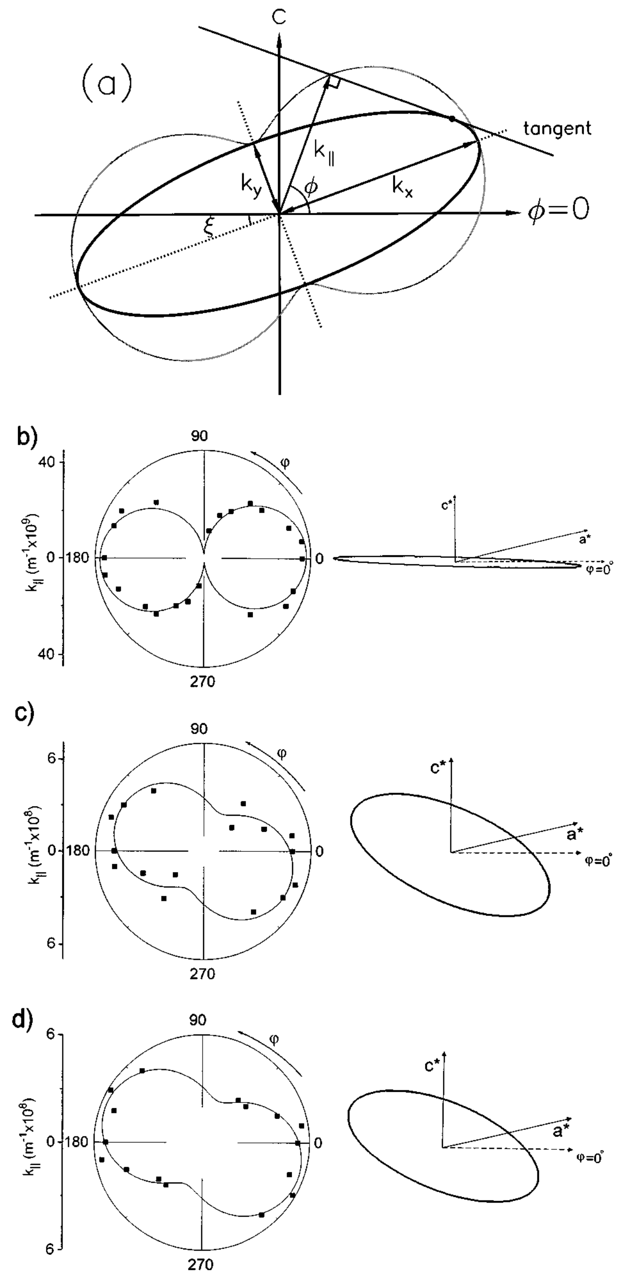

FIG. 7. (a) Elliptical Fermi-surface pocket with its associated dumbbell-like locus formed by the callipered width $k_{\|}$ of the ellipse at the complete range of azimuthal angles φ. Further figures of this form are presented for Fermi-surface pockets derived from the AMRO data: (b) the AMRO near θ=0° at 17 T and 1.5 K, originating from the $F_{\gamma'}\approx$222 T electron pocket, (c) the AMRO near θ=90° at 17 T and 1.5 K, originating from the $F_\alpha\approx$38 T, and (d) the AMRO near θ=90° at 5 T and 1.5 K, originating from the F_α=38 T. Note that the schematic representations of the elliptical Fermi-surface pockets are indicative of the fitted shape and orientation, but are drawn to an arbitrary scale.

vector **a*** (which lies along the direction of the Brillouin zone width), this pocket takes the form shown in Fig. 8.

The AMRO's which occur closer to 90°, both above and below 10 T, can be fitted by a more isotropic Q2D Fermi-surface section, as shown in Figs. 7(c) and 7(d); these figures are derived from AMRO data recorded at 5 and 17 T, respectively, illustrating the field independence of this pocket. The

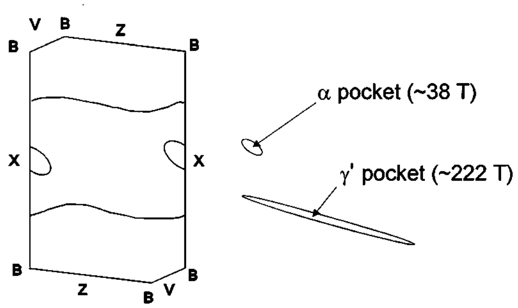

FIG. 8. Direct comparison of the Fermi-surface pockets derived from the experimental data of the present work with the calculated Fermi surface of Mori *et al.* (Ref. 12).

accuracy of the length of the minor axis of a more isotropic Fermi-surface pocket does not depend so much on a high azimuthal resolution. Hence the value obtained for both axis parameters k_y and k_x is much more reliable. From the fit to the 17-T data, we get $k_x=(5.73\pm0.1)\times10^8$ m^{-1}, $k_y=(2.49\pm0.4)\times10^8$ m^{-1}, and $\xi=(-21\pm4)°$, implying that the minor axis of the pocket is rotated by this angle from the crystallographic c axis. The values of k_x and k_y indicate that the area of this Fermi-surface pocket is $S_\alpha=(4.48\pm0.7)\times10^{17}$ m^{-2}, corresponding to a SdH frequency of 47±8 T. A fit to the 5-T data yields $k_x=(6.04\pm0.3)\times10^8$ m^{-1}, $k_y=(2.66\pm0.7)\times10^8$ m^{-1}, and $\xi=(-24\pm7)°$, giving $S_\alpha=(5.05\pm1.3)\times10^{17}$ m^{-2}, which corresponds to a SdH frequency of 53±14 T. This strongly suggests that the α pocket is largely unaffected by any field-induced Fermi-surface reconstruction and that it is associated with the $F_\alpha\approx38$ T SdH frequency present over all field ranges [see Figs. 3, 5(a), and 5(b)].

Support for the above assignments of AMRO features to particular Fermi-surface pockets may be derived from data presented in Ref. 9. The geometrical considerations associated with the observation of AMRO's are also thought to lead to oscillations in the amplitudes of the SdH frequencies[9,18] and this was the technique used in Ref. 9 to derive the approximate Fermi-surface shapes illustrated in Fig. 1(b). Although this method is time consuming and of very limited accuracy [the SdH frequencies disappear at relatively low values of tan(θ) (Ref. 9)], it can potentially lead to a direct association of the Shubnikov–de Haas oscillation frequency with a particular shape of Fermi surface. If one compares Fig. 6 of Ref. 9 with Figs. 7(b)–7(d) of this work, it is apparent that the Fourier amplitude of the 220 T SdH frequency (i.e., $F_{\gamma'}$ in this work) oscillates at small values of θ in a similar manner to the AMRO's which occur only at fields above 10 T whereas the amplitude of the 40 T SdH oscillations (i.e., the F_α series) only begins to oscillate with tilt angle at much higher θ.

However, the limited number of azimuthal angles studied by Doporto *et al.*[9] means that the derived Fermi-surface shapes shown in Fig. 1(b) are only very rough guides; this is especially true for Fermi-surface pockets which are very anisotropic in shape. As a result, Doporto *et al.* obtained areas derived from the angle dependence of the SdH oscillations which they recognized to be too large, and they took this to imply that the SDW nesting vector included an interplane component.[9] The present work illustrates that if AMRO's are recorded at the large number of azimuthal angles necessary to obtain accurate Fermi-surface shapes, then the derived pocket areas agree with the SdH frequencies to within experimental errors; hence, we find that there is no evidence for an interplane component of the SDW nesting vector.

Additional complications affect the method used to derive the Fermi-surface pocket shapes in Ref. 9. The amplitudes of the SdH oscillations of the γ' pocket could have been affected by the background magnetoresistance, which was not taken into account; furthermore, the strong AMRO's of this pocket could partly modulate the SdH oscillations of the other pockets. Other effects, such as a spin zero in the SdH oscillations,[13] could also cause problems by leading to extra minima. It can therefore be concluded that the shapes of the α and γ' Fermi-surface pockets derived in this work are much more reliable than the previous estimates shown in Fig. 1(b).[9]

IV. DISCUSSION

A. Field-induced Fermi-surface changes

The data reviewed in the previous section provide evidence that the Fermi surface of β''-(BEDT-TTF)$_2$AuBr$_2$ undergoes a field-induced change in form between ~10 and ~14 T. At fields below 10 T the Fermi surface appears to be characterized by three small Q2D pockets, which we refer to as α, β, and γ, with areas corresponding to the SdH frequencies $F_\alpha\approx38$ T, $F_\beta\approx143$ T, and $F_\gamma\approx191$ T, respectively. There was speculation in Ref. 9 as to whether the F_β frequency corresponds to a real carrier pocket or whether it results from some kind of frequency mixing effect. However, as is seen in Fig. 4(c), the F_β frequency dominates the SdH oscillations at fields below 6 T, implying that it must be a real Fermi-surface pocket.

At fields above 10 T the F_α frequency persists (as do the associated AMRO's), while the F_β and F_γ frequencies vanish, to be replaced at fields above ~14 T by two new frequencies $F_{\beta'}\approx175$ T and $F_{\gamma'}\approx222$ T; we refer to the associated Fermi-surface pockets as β' and γ', respectively. The AMRO measurements indicate that the γ' pocket is a very elongated ellipse; however, neither the β or γ pockets in the low-field (<10 T) state nor the β' pocket in the high-field state (B>~14 T) results in strong AMRO's. A number of weak features away from the strong α and γ' AMRO's may be perceived in Figs. 6(a) and 6(b), but these were too indistinct for quantitative analysis. The reasons for the nonappearance of Q2D AMRO's have been recently discussed in Ref. 19; it is likely that the β, γ, and β' pockets are too irregularly or severely corrugated to produce oscillations, as the Q2D AMRO effect relies on *weak* and *regular* corrugation of the section of Fermi surface in question.

It is instructive to compare the α and γ' Fermi-surface pockets measured in the high-field state (i.e., deduced from the AMRO's) with the Fermi-surface calculation of Mori *et al.*[12] (Fig. 8). Given the shape of the α pocket and also the fact that it is not affected by any rearrangement of the Fermi surface, we can associate it with the Q2D section predicted by Mori *et al.*, centered on the X point of the Brillouin zone. The size of this pocket is much smaller than the band-structure calculation predictions (derived from room-temperature crystallographic data), implying that a determination of the low temperature crystal structure and improved calculations are required. On the other hand, the elongated γ' pocket is probably generated by the imperfect nesting of the Q1D portions of the Fermi surface. Imperfect nesting should result in at least two pockets and so is likely to be responsible for the β' pocket, which should therefore lie roughly in the same plane as the γ' pocket. From the charge transfer known to occur in the β'' salts, it is expected that the band structure should be exactly three-quarters filled.[9–12] For this reason β''-(BEDT-TTF)$_2$AuBr$_2$ is a compensated semimetallic compound in which the areas corresponding to the occupied and unoccupied states in the first Brillouin zone should be equal. As a result of the SDW, parts of the open pieces of the Fermi surface disappear and the total areas of remaining hole and electron orbits should be equivalent, explaining the approximate additive relationships between the various SdH frequencies (i.e., $F_\alpha + F_{\beta'} \approx F_{\gamma'}$). Taking into account the above consideration for the high-field region in β''-(BEDT-TTF)$_2$AuBr$_2$, we should expect the γ' frequency to be an electron pocket, roughly compensating in area for the α and β' hole pockets. Similar considerations apply in the low-field state below 10 T where the β and γ pockets will result from the imperfect nesting of the Q1D Fermi-surface sections and $F_\alpha + F_\beta \approx F_\gamma$; in this case, γ is expected to be the electron pocket.

We have now provided an interpretation of the abundance of SdH frequencies present in the Fourier transform covering the entire field range (2–60 T); some correspond to the "low-field" (<10 T) Fermi surface, whereas others are due to the "high-field" (>10–14 T) Fermi surface. Only the 53 and 133 T frequencies observed in Fig. 3 have not been accounted for. One possible explanation of these extra frequencies is that they correspond to the maximum (belly) cross section of the α pocket and the minimum (neck) cross section of the β pocket, respectively, resulting from the warping of the Fermi surface in the reciprocal lattice k_b direction; by inspection of Fig. 3, it appears that the frequencies are paired as 38 T with 53 T and 133 T with 145 T. However, if such an interpretation were true, the same splitting should be observable over any magnetic field range provided that the interval in $1/B$ space was sufficiently long to give the Fourier transform an adequate resolution.[13] The lowest magnetic field studies have been performed by Uji *et al.*[10] whose experiments covered the field interval from 2.25 to 13.8 T; this corresponds to a $\sim 0.37\ \mathrm{T}^{-1}$ range in $1/B$, approximately twice that in our pulsed field data. The absence of any splitting of the frequencies in the data of Uji *et al.* suggests two things: first, that the warping of the Fermi surface is not a significant factor in β''-(BEDT-TTF)$_2$AuBr$_2$ and, second, that the apparent splitting of the frequencies is simply an artifact of extending the measurements to very high magnetic fields, probably resulting from the changes in the Fermi surface occurring between 10 and 14 T. The Fourier transform of the region between 10 and 14 T [Fig. 5(a), inset] exhibits a poorly resolved mixture of frequencies, including one close to 133 T. The "split" frequencies are therefore perhaps characteristic of this intermediate transition region between the high-field (>~14 T) and low-field (<~10 T) regimes. Such an extended field width between two different states of a SDW is not without precedent in BEDT-TTF salts; the true width of the "kink" transition between the SDW and metallic states of α-(BEDT-TTF)$_2$KHg(NCS)$_4$ has recently been shown to be ~7 T.[2]

B. Extreme quantum limit

In magnetic fields of 60 T the α frequency reaches the extreme quantum limit where the last Landau level is only partially occupied. The extent to which the last level is occupied will depend on the deviation of the chemical potential μ from its zero-field value. The simple depopulation of a Fermi-surface pocket is usually expected to lead to a reduction in the scattering cross section of the quasiparticles and therefore to an overall drop in the magnetoresistance.[13,20–25] The observed strong increase in the background magnetoresistance at high fields is thus contrary to the expectations of this simple model.

A number of recent theoretical papers[26] have speculated that strong electron self-energy effects will occur as a Q2D metal approaches the extreme quantum limit. This is expected to lead to an enhancement in the density of states (DOS) at the Fermi energy and thus to promote phenomena such as reentrant superconductivity. Given that superconducting and SDW ground states are often found to be competing effects in organic conductors, we might expect the existence of a SDW in β''-(BEDT-TTF)$_2$AuBr$_2$ to prevent superconductivity from taking place. An increase in the DOS at high fields or, alternatively, a reduction of the energy separation of the states could be expected to increase the quasiparticle scattering cross section at high fields and perhaps account for the strong increase in the magnetoresistance which is observed experimentally.

Further evidence for the increase in the DOS at high magnetic fields is found in the values of the quasiparticle effective masses derived from the SdH oscillations over the range from $0.07\ \mathrm{T}^{-1}$ (~14 T) to $0.017\ \mathrm{T}^{-1}$ (~60 T). [Doporto *et al.*[9] evaluated the effective masses in β''-(BEDT-TTF)$_2$AuBr$_2$ at magnetic fields $\leqslant 17$ T, where hysteresis complicates the required analysis of the magnetoresistance; we avoid this problem by evaluating the effective masses at higher magnetic fields.] The standard procedure[13] for extracting the oscillatory component of the magnetoresistance by dividing by the background magnetoresistance $P(1/B)$ was followed, and the temperature dependence of the Fourier amplitude a of the SdH oscillations was fitted to the equation[2,13]

$$a = a_0 X/\sinh X, \tag{3}$$

where

$$X = 2\pi^2 pkT/\hbar\omega_c \approx 14.69 m^* T/B.$$

Table I shows the derived effective masses, which are noticeably higher than the low field (i.e., $\leqslant 17$ T) estimates in Ref. 9. Large effective masses have also been observed in other organic conductors in high magnetic fields[2,8,27,31] and have been attributed to a transition from quasi- to ideal two-dimensional behavior of the quasiparticles with increasing field.[8,27,31] However, recent numerical simulations indicate that the latter effect is unlikely to be responsible for the experimental observations; even in the most extreme case of a zero scattering rate ($\tau^{-1}=0$), the simulations reveal that only the mass estimates of the second and higher harmonics

TABLE I. Effective masses in the high-field state.

$F(T)$	Label	$m^*(m_e)$ $1/B=0.017-0.1\ T^{-1}$
38	α	1.9(3)*
175	β'	4.5(2)
222	γ'	4.0(1)
370	$\beta'+\gamma'-\alpha$	3(1)
404	$\beta'+\gamma'$	4.7(5)
440	$2\gamma'$	4.4(4)

of the quantum oscillations are strongly affected,[28] in agreement with recent experimental data.[2] The process of forcing a fit to the Lifshitz-Kosevich theory[13] to the first harmonic amplitude, even for the most 2D material, does not seem to produce a large deviation in the effective mass estimate.[28] Therefore it is likely that the large effective masses at high magnetic fields shown in Table I signify the presence of an increase in the density of states at high magnetic fields, as predicted by theoretical models.[26]

The invariance of the 38-T frequency over the entire field range enables the quasiparticle scattering rate $\tau^{-1}=0.6\times10^{12}$ s^{-1} to be estimated from the field dependence of the amplitude. This value is comparable to that found for α-(BEDT-TTF)$_2$KHg(SCN)$_4$ in its SDW state.[2] By comparing the Landau-level energy separation $\hbar\omega_c=3.7$ meV with the scattering rate $\hbar\omega_c=0.4$ meV at 60 T, it is apparent that $\omega_c\gg\tau^{-1}$. This condition is the requirement for field-dependent oscillations in the chemical potential μ to become important, and we shall return to this point below.

In fields above ~30 T an apparent splitting of the waveform of the γ' SdH oscillations is observed, probably due to the resolution of Pauli spin splitting of the Landau levels.[13,24] Analysis of the positions of the resistance minima in $1/B$ space reveals that the features are not perfectly periodic. Irregular periodicity is often encountered in 2D semiconductor systems with very sharply defined Landau levels (i.e., $\omega_c\gg\tau^{-1}$) when the quantum limit is approached,[25,29] as the carriers redistribute themselves among the Fermi-surface pockets (subbands) in order to conserve their total number. As a result, the oscillations of the chemical potential μ become progressively more irregular as the extreme quantum limit is approached. The largest observed SdH frequency (γ' pocket) in β''-(BEDT-TTF)$_2$AuBr$_2$ has only three or four Landau levels remaining at 60 T, and so it would be expected that these effects should be significant. This behavior is similar to the magnetic interaction in that it can lead to a strong harmonic content and to sum and difference frequencies in the Fourier spectrum.[13,25,29] Several sum and difference frequencies are indeed observed in the Fourier transform in Fig. 5(a); note that the corresponding "effective masses" (Table I) do not correspond to simple sums of the effective masses of the various frequency components, indicating that the sum and difference frequencies observed cannot be due to magnetic breakdown.[13,30] The values and amplitudes of the frequencies present, in particular the presence of a strong $F_{\beta'}+F_{\gamma'}$ sum frequency, give additional evidence that both the $F_{\beta'}$ and $F_{\gamma'}$ frequencies correspond to real carrier pockets. The latter sum frequency would not be present if the $F_{\beta'}$ frequency was itself generated by frequency mixing effects. In contrast, below 10 T [Fig. 5(b)] there is no evidence for any frequency mixing.

In a 2D or Q2D system at high magnetic fields and sufficiently low temperatures, the magnetoresistance oscillations should begin to exhibit sharp maxima.[28] This effect has been observed in other organic salts.[3,8,15,27] The sharp minima observed in β''-(BEDT-TTF)$_2$AuBr$_2$ therefore contrast with the simple behavior expected, and the reasons for this are as yet unclear.

V. CONCLUSION

Single crystals of β''-(BEDT-TTF)$_2$AuBr$_2$ have been studied using pulsed magnetic fields of up to 60 T and angle-dependent magnetoresistance oscillation (AMRO) measurements carried out in quasistatic fields. The strong temperature dependence of the magnetoresistance of β''-(BEDT-TTF)$_2$AuBr$_2$ and the persistence of several Shubnikov–de Haas (SdH) frequencies at fields of up to 60 T indicate that the spin density wave (SDW) previously noted in this material[9] persists to the highest available fields. Both the SdH oscillations in the magnetoresistance and the AMRO measurements show that two distinct phases, each with a characteristic Fermi surface, exist within this SDW state; these correspond to magnetic fields of <~10 T and magnetic fields >~14 T, respectively, and are separated by an apparently extended transition region between ~10 and ~14 T. The Fermi surface in the low-field regime consists of three pockets α, β, and γ, with areas corresponding to the SdH frequencies $F_\alpha\approx38$ T, $F_\beta\approx143$ T, and $F_\gamma\approx191$ T. Above 14 T the AMRO measurements show that the α pocket is unaltered, indicating that it probably corresponds to the closed quasi-two-dimensional (Q2D) Fermi-surface section in the calculations of Mori *et al.*[12] In contrast, above 14 T the β and γ Fermi-surface sections are replaced by β' and γ' pockets, with areas corresponding to SdH frequencies $F_{\beta'}\approx175$ T and $F_{\gamma'}\approx222$ T. The β, γ, β', and γ' pockets probably result from imperfect nesting of Q1D sections of the high-temperature Fermi surface; support for this assignment is given by the AMRO measurements, which show that the γ' pocket is very elongated with its long axis parallel to the crystallographic a direction.

At magnetic fields approaching 60 T, a strong increase in the magnetoresistance and larger effective masses than those measured at low fields are observed, perhaps indicating that the density of states is enhanced as a result of the approach of the ultraquantum limit. The Landau levels in this field region appear to be very sharply defined so that mixing of the Shubnikov–de Haas frequencies occurs due to strong oscillations of the chemical potential.

ACKNOWLEDGMENTS

This work is supported by EPSRC (UK), the Royal Society (UK), and the European Union HCM, TML, and Large Facility Programs. The Leuven Laboratory is supported by the National Fonds voor Wetenschappelijk Onderzoek. A.H. wishes to thank the Erasmus program for financial support. N.H. is supported by the Onderzoeksraad, K. U. Leuven. We should like to thank Professor G. Pitsi and Professor C. Agosta for provision of components for the ^{3}He cryostat, and Dr. S. Uji for fruitful discussions.

[1] J. Singleton, F. L. Pratt, M. Doporto, J. M. Caulfield, S. O. Hill, T. J. B. M. Janssen, I. Deckers, G. Pitsi, F. Herlach, W. Hayes, J. A. A. J. Perenboom, M. Kurmoo, and P. Day, Physica B **184**, 470 (1993).

[2] N. Harrison, A. House, I. Deckers, J. Caulfield, J. Singleton, F. Herlach, W. Hayes, M. Kurmoo, and P. Day, Phys. Rev. B **52**, 5584 (1995).

[3] P. S. Sandhu, G. J. Athas, J. S. Brooks, E. G. Haanappel, J. D. Goette, D. W. Rickel, M. Tokumoto, N. Kinoshita, T. Kinoshita, and Y. Tanaka (unpublished).

[4] T. Osada, R. Yagi, A. Kawasumi, S. Kagoshima, N. Miura, M. Oshima, and G. Saito, Phys. Rev. B **41**, 5428 (1990).

[5] J. Singleton, J. M. Caulfield, S. O. Hill, P. T. J. Hendriks, F. L. Pratt, M. Doporto, I. Deckers, G. Pitsi, F. Herlach, W. Hayes, T. J. B. M. Janssen, J. A. A. J. Perenboom, M. Kurmoo, and P. Day, in *Proceedings of Conference Physique en Champs Magnétiques Très Intenses et Technologies Associées*, Toulouse, 1993, edited by J. Leotin (CNRS-UPS-INSA, Toulouse, 1993), p. J2-1.

[6] J. S. Brooks, C. C. Agosta, S. J. Klepper, M. Tokumoto, N. Kinoshita, H. Anzai, S. Uji, H. Aoki, A. S. Perel, G. J. Athas, and D. A. Howe, Phys. Rev. Lett. **69**, 156 (1992); A. M. Gerrits, T. J. B. M. Janssen, A. S. Perel, J. S. Brooks, A. Wittlin, J. A. A. J. Perenboom, and P. J. M. van Bentum, Synth. Met. **70**, 735 (1995) and references therein.

[7] T. Sasaki and N. Toyota, Phys. Rev. B **49**, 10 120 (1994).

[8] P. S. Sandhu, G. J. Athas, J. S. Brooks, E. G. Haanappel, J. D. Goettee, D. W. Rickel, M. Tokumoto, N. Kinoshita, T. Kinoshita, and Y. Tanaka (unpublished).

[9] M. Doporto, J. Singleton, F. L. Pratt, J. Caulfield, W. Hayes, J. A. A. J. Perenboom, I. Deckers, G. Pitsi, M. Kurmoo, and P. Day, Phys. Rev. B **49**, 3934 (1994).

[10] S. Uji, H. Aoki, M. Tokumoto, A. Ugawa, and K. Yakushi, Physica B **194**, 1307 (1994).

[11] M. Tokumoto, A. G. Swanson, J. S. Brooks, C. C. Agosta, S. T. Hannahs, N. Kinoshita, H. Anzai, M. Tamura, H. Tajima, N. Kuroda, A. Ugawa, and K. Yakushi, Physica B **184**, 508 (1993); **184**, 508 (1993).

[12] T. Mori, F. Sakai, G. Saitoh, and H. Inokuchi, Chem. Lett. **1986**, 1037 (1986).

[13] D. Shoenberg, *Magnetic Oscillations in Metals* (Cambridge University Press, Cambridge, England, 1984).

[14] F. Herlach, M. van der Burgt, I. Deckers, G. Heremans, G. Pitsi, and L. van Bockstal, Physica B **63**, 177 (1992).

[15] J. Caulfield, S. J. Blundell, M. S. L. du Croo de Jongh, P. T. J. Hendriks, J. Singleton, M. Doporto, F. L. Pratt, A. House, J. A. A. J. Perenboom, W. Hayes, M. Kurmoo, and P. Day, Phys. Rev. B **51**, 8325 (1995).

[16] J. S. Brooks, X. Chen, S. J. Klepper, S. Valfells, G. J. Athas, Y. Tanaka, T. Kinoshita, N. Kinoshita, M. Tokumoto, H. Anzai, and C. C. Agosta, Phys. Rev. B **52**, 14 457 (1995); S. Uji, T. Terashima, H. Aoki, J. S. Brooks, M. Tokumoto, N. Kinoshita, T. Kinoshita, Y. Tanaka, and H. Anzai, J. Phys. Condens. Matter **6**, L539 (1994); M. V. Kartsovnik, H. Ito, T. Ishiguro, H. Mori, T. Mori, G. Saito, and S. Tanaka, *ibid*. **6**, L479 (1994).

[17] In the very-low-field studies of Uji *et al.* (Ref. 10), further higher frequencies have been observed in the Fourier spectra, which have been accounted for as sum and difference frequencies of the lower peaks present. It has been proposed that these frequencies result from the Shoenberg magnetic interaction, but in the light of recent evidence (Ref. 2), it is clear that an alternative explanation must be sought. Sum frequencies could result from magnetic breakdown or could possibly arise from the application of the field-modulation technique over a region of the magnetoresistance where it is known to be strongly hysteretic.

[18] M. V. Kartsovnik, V. N. Laukhin, S. I. Pesotskii, I. F. Schegolev, and V. M. Yakovenko, J. Phys. (France) I **2**, 89 (1992); K. Yamaji, J. Phys. Soc. Jpn. **58**, 1520 (1989).

[19] S. J. Blundell and J. Singleton, Phys. Rev. B **53**, 5609 (1996).

[20] X. D. Shi, W. Kang, and P. M. Chaikin, Phys. Rev. B **50**, 1984 (1994); N. A. Fortune, J. S. Brooks, M. J. Graf, G. Montambaux, L. Y. Chiang, J. A. A. J. Perenboom, and D. Althof, Phys. Rev. Lett. **64**, 2054 (1990); R. C. Yu, L. Chiang, R. Upasani, and P. M. Chaikin, *ibid*. **65**, 2458 (1990).

[21] X. Yan, M. J. Naughton, R. V. Chamberlin, S. Y. Hsu, L. Y. Chiang, J. S. Brooks, and P. M. Chaikin, Phys. Rev. B **36**, 1799 (1987).

[22] R. G. Clark (private communication).

[23] K. Kajimura, H. Tokumoto, M. Tokumoto, K. Murata, T. Ukachi, H. Anzai, T. Ishiguro, and G. Saito, J. Phys. (Paris) Colloq. **44**, C3-1059 (1983); S. Uji (private communication).

[24] F. L. Pratt, J. Singleton, M. Doporto, A. J. Fisher, T. J. B. M. Janssen, J. A. A. J. Perenboom, M. Kurmoo, W. Hayes, and P. Day, Phys. Rev. B **45**, 13 904 (1992).

[25] M. J. Kelly and R. J. Nicholas, Rep. Prog. Phys. **40**, 1699 (1985); J. Singleton, F. Nasir and R. J. Nicholas, Proc. SPIE **659**, 99 (1986).

[26] See, e.g., H. Goto and Y. Natsume, J. Phys. Soc. Jpn. **63**, 1465 (1994) and references therein.

[27] P. Christ, W. Biberacher, A. G. M. Jansen, M. Kartsovnik, A. Kovalev, N. Kushch, E. Steep, and K. Andres (unpublished); Surf. Sci. (to be published).

[28] N. Harrison, R. Bogaerts, P. Reinders, J. Singleton, S. J. Blundell, and F. Herlach (unpublished).

[29] R. M. Kusters, J. Singleton, G. Gobsch, G. Paasch, D. Schulze, F. Wittekamp, G. A. C. Jones, J. E. F. Frost, D. C. Peacock, and D. A. Ritchie, Superlatt. Microstruct. **9**, 55 (1991); R. M. Kusters, F. A. Wittekamp, J. Singleton, J. A. A. J. Perenboom, G. A. C. Jones, J. E. F. Frost, D. C. Peacock, and D. A. Ritchie, Phys. Rev. B **46**, 10 207 (1992).

[30] J. M. Caulfield, J. Singleton, F. L. Pratt, M. Doporto, W. Lubczynski, W. Hayes, M. Kurmoo, P. Day, P. T. J. Hendriks, and J. A. A. J. Perenboom, Synth. Met. **61**, 63 (1993).

[31] V. N. Laukhin, A. Audouard, H. Rakoto, J. M. Broto, F. Goze, G. Coffe, L. Brossard, J. P. Redoules, M. V. Kartsovnik, N. D. Kusch, L. I. Buravov, A. G. Khomenko, E. B. Yagubskii, S. Askenazy, and P. Pari, Physica B **211**, 282 (1995).